

**Caltech Faint Galaxy Redshift Survey XV:
Classifications of Galaxies with $0.2 < z < 1.1$ in the Hubble Deep
Field (North) and its Flanking Fields ¹**

Sidney van den Bergh

Dominion Astrophysical Observatory, Herzberg Institute of Astrophysics, National
Research Council of Canada, 5071 West Saanich Road, Victoria, BC, Canada V9E 2E7

sidney.vandenbergh@nrc.ca

Judith G. Cohen

Palomar Observatory, Mail Stop 105-24, California Institute of Technology, Pasadena, CA
91125

jlc@astro.caltech.edu

and

Christopher Crabbe

California Institute of Technology, Mail Stop 185-54, Pasadena, CA 91125

crabbe@its.caltech.edu

Received _____; accepted _____

ABSTRACT

To circumvent the spatial effects of resolution on galaxy classification, the images of 233 objects of known redshift in the Hubble Deep Field (HDF) and its Flanking Fields (FF) that have redshifts in the range $0.20 < z < 1.10$ were degraded to the resolution that they would have had if they were all located at a redshift $z = 1.00$. As in paper XIV of the present series, the effects of shifts in rest wavelength were mitigated by using R -band images for the classification of galaxies with $0.2 < z < 0.6$ and I -band images for objects with redshifts $0.6 < z < 1.1$. A special effort was made to search for bars in distant galaxies. The present data strongly confirm the previous conclusion that the Hubble tuning fork diagram only provides a satisfactory framework for the classification of galaxies with $z < 0.3$. More distant disk galaxies are often difficult to shoehorn into the Hubble classification scheme. The paucity of barred spirals and of grand-design spirals at large redshifts is confirmed. It is concluded that the morphology of disk galaxies observed at look-back times smaller than 3–4 Gyr differs systematically from that of more distant galaxies viewed at look-back times of 4–8 Gyr. The disks of late-type spirals at $z > 0.5$ are seen to be more chaotic than those of their nearer counterparts. Furthermore the spiral structure in distant early-type spirals appears to be less well-developed than it is in nearby early-galaxies.

Subject headings: galaxies:evolution, galaxies:formation, surveys

¹Based in part on observations obtained at the W.M. Keck Observatory, which is operated jointly by the California Institute of Technology and the University of California

1. Introduction

The Hubble Space Telescope has, for the first time, allowed us to undertake systematic imaging surveys (Williams *et al.* 1996) of galaxies at large redshifts. Furthermore, spectra obtained with the W. M. Keck 10-m telescope (Cohen *et al.* 2000) have made it possible to determine redshifts (and hence look-back times) for significant numbers of such distant galaxies. In recent papers (van den Bergh *et al.* 1996, 2000; Binchmann *et al.* 1998)² it was found that disk galaxies at redshifts $\gtrsim 0.3$ have morphologies that appear to differ systematically from those of nearby galaxies. A question that presents itself quite insistently is: Could the decrease in linear resolution with increasing distance contribute significantly to these apparent systematic changes of morphology with redshift? In an attempt to answer this question we have degraded the images of all galaxies with redshifts 0.20 to 1.00 to the appearance that they would have had at $z = 1.00$. (The images of 20 galaxies with $1.0 < z < 1.1$ were left unaltered.) As has already been discussed in van den Bergh *et al.* (2000) (henceforth vdB2000), all galaxies were classified at similar rest wavelengths by comparing *R*-band images of galaxies having $0.20 < z < 0.60$ with *I*-band images of objects having $0.60 < z < 1.10$. For statistical purposes the present data may be compared with the *B*-band images of galaxies with $z \sim 0.0$ that are seen on the Palomar Sky Survey. The redshifts for individual HST + FF galaxies in the present paper are from Cohen *et al.* (2000) and Cohen (2001). Since only a single redshift was available for five merging/interacting galaxies the total number of images of galaxies examined (233) is slightly larger than the total number of redshifts (228).

For more detailed references to previous work on the morphology and classification of

²Binchmann *et al.* (1998) classify galaxies with respect to nine fundamental type standards. One of us (SvdB) would have classified their Sbc standard as Sb, their Scd standard as Sc I and their Ir standard (which appears to have a central nucleus) as a spiral.

distant galaxies the reader is referred to the excellent review by Abraham (1999).

2. Effects of Resolution and of Noise

“Postage stamp” images of every individual galaxy with $0.20 < z < 1.00$ were manipulated in both brightness and in angular scale to mimic the appearance that they would have had at $z = 1.00$. The images of galaxies with $1.00 < z < 1.10$ were left untouched. For $z < 0.6$ the HST F606W images were used, while the F814W images were employed for those galaxies in the sample with $z > 0.6$. For many of the galaxies in the Flanking Fields, no F606W images were available. These objects were therefore omitted from the present study.

The angular scale for each galaxy with $z < 1.00$ was compressed by a factor $f =$ (observed angular diameter) / (angular diameter at $z = 1.00$), using a cosmology with $H_0 = 60 \text{ km s}^{-1} \text{ Mpc}^{-1}$ and $\Omega_M = 0.3$. We then corrected the intensity in the F606W images to take into account the wavelength dependence of the difference in photon detection efficiency between the WFPC2 instrument behind the F606W and F814 filters. Finally each image with $z < 1.00$ was dimmed by a factor $S = [D_L(z = 1)/D_L(z)]^2$. Furthermore we took into account the dependence on rest wavelength of the spectral energy distribution of a galaxy; such objects are typically much brighter at 7500 \AA in the rest frame than they are at 4050 \AA .

The procedure outlined above also suppresses the noise in the subimage arising from instrumental contributions and from the sky by the same factor S , which for low redshifts may be quite significant. At this point the contrast between the galaxy and the background is artificially enhanced. To restore the proper noise level, a set of images consisting of random realizations of the noise characteristics of the F606W images in the three WF CCDs

and in the PC were generated. These were derived from the noise properties measured in the original HST images in regions apparently free of galaxies. Then, for galaxies with $z < 0.6$, these were added appropriately to the compressed and rescaled images.³ This then creates a set of “postage stamp” images in which each galaxy appears as it would if that object were situated at $z = 1.0$ in the image in which it was originally observed.

Comparison of the new images with those used in vdB2000 showed no cases in which our original classifications had to be revised. The only (quite subtle) difference was that faint, possibly tidal, features in the outer parts of some images were more difficult to see than they had been in the original images. No significant differences were seen between the morphologies of the main bodies of our program galaxies before, and after, an appropriate amount of noise had been added. It is therefore concluded that the classifications of vdB2000 are robust with regard to reasonable changes in the noise level.

3. Classification of the Images

Table 1 lists the galaxies for which images degraded to $z = 1.00$ were available from the survey of Cohen *et al.* (2000) augmented in Cohen (2001). In an attempt to search for weak bars these images were scrutinized over a larger dynamical range than had previously been explored for the classifications given in vdB2000. Classifications for all objects were made by SvdB and are given on the DDO system (van den Bergh 1960a,b,c). This system is close to that adopted by Sandage & Tammann (1981). The main difficulty encountered during the classification process was that a significant fraction of the galaxies at large

³In principle this should have been done for the “postage stamps” with $0.6 < z < 1.0$ as well, but tests on the lower redshift subimages showed that restoring the correct noise level had no significant effect for our purposes.

redshifts look “odd” and were therefore often difficult (or impossible) to shoehorn into the classification bins of the Hubble system. For such objects a “p” (peculiar) was added to their classifications. Since spiral structure in distant galaxies, which are viewed at large look-back times, is less developed than it is in nearby galaxies, the morphology of spiral arms often can not be used as a classification parameter. Central concentration of light was therefore often used as the primary classification criterion for determining where a spiral galaxy is located on the Sa – Sb – Sc sequence. Inspection of the present images that were degraded to their appearance at $z = 1.00$ strengthens and confirms the previous conclusion (van den Bergh *et al.* 1996, 2000) that the morphology of late-type disk galaxies at large look-back times is more chaotic than that of nearer spirals of types Sbc – Sc. In distant early-type disk galaxies the spiral arms are seen to be less developed than they are in nearby Sa – Sb galaxies. As the images used to derive this conclusion had all been degraded to $z = 1.0$, the observed decrease in the strength of spiral structure with increasing z cannot be a resolution effect.

The surface density of galaxy images at the depth of the HST images of the HDF and FF is quite high. As a result, these fields contain many apparent close pairs of galaxies, several of which were shown in our previous paper to have widely discrepant redshifts, and hence are established as chance projections. Because of this high probability of finding chance pairs we have, whenever practicable, used tidal deformation of images as a criterion for assigning objects to the “merger” class. Because we have been more conservative in designating objects to this class the fraction of “mergers” is smaller than it was in vdB2000.

Our work provided many examples of late-type galaxies at high redshifts that appeared to be in a very early evolutionary state. With growing experience we have therefore become more confident in assigning objects to the “proto-Sc” class. This classification type is therefore now more common than it was in our previous paper. As a result some objects

previously dubbed “Sc pec” have now been reclassified as “proto-Sc”.

The fact that galaxies at large redshifts appear so odd, and are difficult to fit into the Hubble scheme, adds significantly to the uncertainty of assigned Hubble types. It is therefore a source of satisfaction to find such good agreement between our original classifications of individual galaxies in vdB2000 and the present classifications of images of these same objects degraded to $z = 1.0$. A blind comparison between the present new classifications of 99 objects that could be placed on the Hubble sequence E–Sa–Sb–Sc–Ir, and those which were previously published for these same objects in vdB2000 shows exact agreement for 49 objects, a difference of 0.5 Hubble class for 23 objects, a difference of 1.0 Hubble class for 23 objects and a difference > 1.0 Hubble class for 4 objects. For three of these four discrepant classifications the cause appears to have been that a small fraction of the images classified in vdB2000 were not inspected over a sufficiently large dynamic range.

For this sample in common of 99 galaxies that could be placed on the Hubble sequence E–Sa–Sb–Sc–Ir there is thus no evidence for any systematic difference in Hubble type between the old classifications and the new classifications of images degraded to $z = 1.0$. Furthermore, there is no evidence for any systematic dependence of the differences between the old and new classifications on redshift. Among 56 galaxies with $0.20 < z < 0.80$ the mean difference, in the sense old type minus new type, is found to be -0.04 ± 0.11 Hubble classes. For the 41 galaxies on the Hubble sequence with $0.80 < z < 1.10$, the mean difference, in the sense old type minus new type, is -0.08 ± 0.12 Hubble classes. Furthermore, the differences between old and new classification types does not appear to depend in a systematic way on Hubble type. On the basis of these results it is concluded that there are no significant differences between Hubble types assigned in vdB2000 and those of degraded images in the present study. A tabulation of the frequencies of various classification types of galaxies in Table 1 as a function of redshift is shown in Table 2.

4. Galaxy Statistics

4.1. Frequency of Barred Galaxies

It was first noted that barred spirals appear to be deficient among galaxies at high redshift by van den Bergh *et al.* (1996). Subsequently this shortage of barred objects at $z > 0.5$ was confirmed (in both the northern and in the southern HDF) by Abraham *et al.* (1999). Bothun (2000) suspected that the absence of SB galaxies at high redshifts might have been due to bandshift effects that result from the fact that bars appear to be more frequent in the *I*-band (Eskridge *et al.* 2000) than they are in the *B*-band. However, the observations of bar frequencies at various redshifts by vdB2000, which were obtained at almost constant rest wavelength, appear to rule out this explanation.

In the present investigation special attention was paid to the possible presence of bars by inspecting each program galaxy over the widest possible dynamic range. Out of 233 images, only a single one was found to be a pure barred spiral of type SB, while one was an intermediate type object classified as S(B). Furthermore three galaxies were classified S(B?). The corresponding percentages are 0.4% SB, 0.4% S(B) and 1.3% S(B?), respectively. For comparison, Sandage & Tammann (1981) found that 22% of all Shapley-Ames galaxies, which have $z \sim 0.0$, are barred. These data suggest that the fraction of all galaxies that are barred is at least an order of magnitude lower in the distant HDF + FF sample than it is in the nearby Shapley-Ames sample. It is noted in passing that the only two certain barred galaxies in the present sample [which were classified SB and S(B)] have $z < 0.5$. Nevertheless, it is puzzling that the fraction of barred spirals at all redshifts appears to be so much lower on HST images than it is on photographs of nearby galaxies. Simulations to investigate this problem are currently being undertaken by Abraham & van den Bergh (in preparation).

Since the Universe is expanding, galaxies were once closer together than they are at the present time. As a result, tidal interactions and mergers are expected to be more frequent at high redshifts than they are at the present time. Evidence based on galaxy morphology in favor of this view was first provided by observations of galaxies in the Hubble Deep Field (van den Bergh *et al.* 1996). Possibly the high frequency of tidal interactions in the early universe also contributed to the shortage of large well-developed disks in galaxies at $z \gg 1$, which was already noted above. Using the present (rather strict) definition of mergers, the data in Table 2 show that 11 out of 116 (9%) of all galaxies with $0.70 < z < 1.00$ are classified as either “Merger” or “Peculiar/merger”. From inspection of the entire data set, one of us (SvdB) has the impression that the rate of multiple mergers may be increasing faster with redshift than the rate of binary mergers.

4.2. Changes in the Relative Frequencies of Galaxy Types as a Function of Redshift

Table 2 shows the frequency distributions of different morphological types in the present sample as a function of redshift. The data in this table may be compared to those of the northern Shapley-Ames galaxies (van den Bergh 1960c) given in vdB2000. The Shapley-Ames galaxies, which are located at $z \sim 0.0$, were classified on reproductions of the B images of the Palomar Sky Survey. They have therefore been observed at approximately the same rest wavelength as the HST images of galaxies with $z > 0.20$. Since galaxies of types E, Sa and Sb have rather similar luminosity functions their relative frequencies (as a function of redshift) should not be strongly affected by redshift-dependent selection effects. However, the present luminosities of late-type spirals are, on average, significantly lower than those of galaxies having earlier Hubble types [see Fig. 1 of van den Bergh (1998)]. In the absence of evolutionary effects, high-redshift samples of galaxies might therefore be

biased against objects of types Sc and Ir. It should, however, be emphasized that this bias against late-type galaxies will be lessened (or might even be reversed) if such objects exhibit significant luminosity evolution. Lilly *et al.* (1995) and Cohen (2000) have, for example, demonstrated that galaxies with $0.5 < z < 0.75$ might have brightened by as much as 1 mag. On the other hand, Carollo & Lilly (2001) have more recently noted that the high metallicity of late-type galaxies with $0.5 < z < 1.0$ makes it improbable that these objects are luminosity-enhanced dwarfs.

The data in Table 2 suggest that the fraction of late-type (Sc + Sc/Ir + Ir) galaxies decreases with increasing redshift. For the redshift bins $z = 0.20 - 0.49$, $0.50 - 0.79$ and $0.80 - 1.09$ the percentage of late-type galaxies is found to be 19%, 12% and 8%, respectively. Taken at face value, this trend suggests that the fraction of late-type galaxies decreases with increasing redshift. Such an effect could, if real, be explained by assuming that a large fraction of all Sc galaxies have not yet been fully assembled, or are still classified as “proto-Sc”, at $z > 0.5$. Alternatively, if luminosity evolution is unimportant, this effect might be due to a distance-dependent selection effect which results from the fact that late-type galaxies are (on average) less luminous than early-type galaxies [see Fig. 1 of van den Bergh (1998)].

The present sample is so small that bins containing objects in a small range of redshifts and morphological types provide pitifully small statistical samples of galaxies. Furthermore the distribution of morphologies at a given redshift might be affected by density enhancements as the line of sight passes through sheets or clusters of galaxies. Intersection of the line of sight towards the HDF with a populous group of galaxies at $z \sim 0.68$ is, for example, responsible for an excess of E galaxies in the $z = 0.60 - 0.69$ redshift bin. As a result of the vagaries of small-number statistics, and the effects of local density enhancements on galaxy morphology, it would be unwise to draw very strong

conclusions from the present data about the morphological evolution of galaxies over time.

The apparent increase in the number of ellipticals with $z > 0.9$ might be spurious, even if it is not due to the vagaries of small number statistics. This is so because any small compact high surface brightness object with regular oval isophotes will be classified as an “elliptical”. This includes the class of galaxies denoted as “blue compact galaxies” [see, for example, Phillips *et al.* (1997), Guzmán *et al.* (1997)], a local example of which might be NGC 6789. These two groups are not easily distinguished morphologically in this redshift regime. However, from the spectra and SEDs of the set of galaxies under consideration here given in earlier papers in this series, we are confident that many of these galaxies are not classical ellipticals, but are instead strongly star forming blue galaxies which are compact.

5. Morphological Evolution of Galaxies

Since the majority of elliptical galaxies are believed to have formed at $z > 1.0$, the present galaxy sample is not expected to contain many proto-ellipticals. Nevertheless, some compact pairs and groupings of early-type galaxies might, in the fullness of time, merge into run-of-the-mill ellipticals. A few E and Sa galaxies in the present sample exhibit faint chaotic outer structures that might have resulted from such earlier mergers.

Many of the early-type (Sa, Sab) spirals in our sample exhibit morphological peculiarities. The most common of these are: (1) underdeveloped spiral structure, (2) warped disks and (3) off-center nuclear bulges. A large fraction of the late-type (Sbc, Sc, Sc/Ir) galaxies in our sample of high redshift galaxies exhibit morphological peculiarities that distinguish them from their nearby counterparts. The disks of distant Sc galaxies tend to be much more chaotic than those of nearby luminous galaxies which generally exhibit a well-ordered spiral structure. This effect is particularly significant because the

sample of distant late-type galaxies is biased in favor of objects of above-average luminosity. Such galaxies are expected (van den Bergh 1960a) to exhibit particularly long and regular spiral arms. Distant single Sc spirals sometimes have one strongly dominant spiral arm. Among nearby galaxies such single-arm objects are usually objects that have been tidally perturbed. Furthermore, the disks of proto-Sc galaxies, in which spiral structure is not yet well developed, are often seen to contain luminous blue knots (super-associations). In other words, huge localized bursts of star formation appear to occur before a well-ordered spiral pattern develops. If the regions in which such super-associations occur have significant overdensities they could experience strong dynamical friction and spiral towards the galactic center (Noguchi 1998), where they might contribute to the formation of a galactic bulge.

Figure 1 shows a good example of an Sc I galaxy at $z = 1.01$ that is just beginning to form well-ordered spiral structure. Note that the arms of this object are much patchier and more chaotic than those of typical nearby Sc I galaxies. The luminous patches (super-associations) in this object are seen to be much more luminous than those that occur in typical Sc I galaxies at $z \sim 0.0$. A color image of an even more primitive late-type galaxy is shown as Plate 9 of van den Bergh *et al.* (1996). This object exhibits what appears to be a disk, in which 10 bright blue knots (super-associations) are embedded. A single slightly off-center red knot may be the (slightly older) nuclear bulge of this probable protogalaxy. Figure 2 shows an example of an object at $z = 1.06$ that might be a proto-Sc with a single arm that contains a super-association. Alternatively this object might be interpreted as the final phase of a merger. Spectroscopic observations will be required to distinguish between these two alternatives. Finally, Figure 3 shows what may be another example of a proto-galactic disk in which a nucleus, and four other bright knots, appear to be embedded.

6. Conclusions

The present data have allowed us to study the evolution of galaxy morphology over the range $0.2 < z < 1.1$ at an effective wavelength that is insensitive to redshift, and at a spatial resolution that is independent of z . The main conclusion that can be drawn from this work is that the morphology of disk galaxies has evolved rapidly over the last 8 Gyr. At look-back times > 4 Gyr, late-type spirals generally have a much more chaotic structure than do nearby galaxies of type Sbc and Sc. Furthermore, the arms of such distant spirals tend to be patchy and are also often asymmetric. At look-back times > 4 Gyr, early-type spiral galaxies appear to have less well-developed spiral structure than do their counterparts that are viewed at look-back times of less than 3–4 Gyr. Apparently, insufficient time was available for spiral structure to develop in such early-type galaxies. Among distant galaxies in the Hubble Deep Field the intrinsic frequency of barred spirals appears to be at least an order of magnitude lower than it is for nearby galaxies at $z \sim 0$. It is concluded that the Hubble (1936) tuning fork scheme is only appropriate for the classification of galaxies at $z < 0.3$ which are viewed at look-back times of less than 3–4 Gyr.

We are indebted to Roger Blandford and to David Hogg for their assistance and advice during the course of the present investigation. We also thank Bob Abraham for his help with the figures.

Table 1. CLASSIFICATIONS OF GALAXIES

ID ^a	Redshift ^b	R^c (Mag)	Classification	Comments
F36438_1357	0.201	20.65	Sb:	On edge of image
F36510_0938	0.205	21.27	Ir	Edge-on
F36545_1014	0.224	23.86	Sa	
H36560_1329	0.271	23.80	Ir	
H36580_1300	0.320	22.04	Sabp(t?)	Double nucleus
F36563_1209	0.321	23.22	Sb - Ir	Edge-on
H36470_1236	0.321	20.62	Sb:p	
H36587_1252	0.321	20.99	SBcp	One long arm
H36508_1255	0.321	22.27	Sp	Edge-on
H36551_1311	0.321	23.58	Merger?	
F36458_1325	0.321	20.71	Scp	Rudimentary spiral structure
H36526_1219	0.401	23.11	E4p	Embedded in asymmetric nebulosity
H36516_1220	0.401	21.45	Sabp	Binary nucleus
F36410_0949	0.410	20.38	Ir/Merger?	
H36472_1230	0.421	22.63	S(B?)bp	Edge-on
H36419_1205	0.432	20.82	Scp	
H36513_1420	0.439	23.22	Sb(?)p	
F36454_1325	0.441	22.33	Sap	Asymmetric

Table 1—Continued

ID ^a	Redshift ^b	R^c	Classification	Comments
		(Mag)		
H36465_1203	0.454	24.32	?	Tidal debris?
H36429_1216	0.454	20.51	Sc I:	
H36448_1200	0.457	22.85	Sbc _p	Rudimentary spiral structure
H36519_1209	0.458	22.75	Sp(t?)	
H36594_1221	0.472	23.53	Sa + Sp	Spectrum probably refers to combined light
H36501_1239	0.474	20.43	Sc?p	Binary nucleus
H36569_1302	0.474	23.69	E0/star	
H36496_1257	0.475	21.91	Pec	Compact and asymmetric
H36572_1259	0.475	21.07	S(B)cp	Perhaps proto?-SBc
H36497_1313	0.475	21.46	Sbp	Asymmetric
H36480_1309	0.476	20.43	E0p	Asymmetric envelope
H36493_1311	0.477	21.97	E2	
H36415_1200	0.483	25.03	Pec	
H36508_1251	0.485	23.15	proto-Sc	
F36446_1304	0.485	21.14	Sbp	Proto-Sb?
F36427_1306	0.485	22.02	Sab	Edge-on
H36528_1404	0.498	23.45	Pec/Merger	

Table 1—Continued

ID ^a	Redshift ^b	R^c	Classification	Comments
		(Mag)		
H36465_1151	0.503	22.00	E0	
F36397_1009	0.509	21.59	Sbp	Asymmetric
H36549_1314	0.511	23.81	?	Edge-on
H36489_1245	0.512	23.48	Ir:	
H36536_1417	0.517	23.36	Sab/S0	Edge-on
F36516_1052	0.518	23.04	Ir	
H36566_1245	0.518	20.06	Sbp	Smooth disk with little star formation
F36213_1417	0.520	20.73	Sa	
H36569_1258	0.520	23.84	E5/Sa	
F36425_1518	0.533	21.79	Sbc	
H36414_1142	0.548	23.51	Merger	Merger of Sap + Sap + ? + Sab:
F36429_1030	0.551	21.82	E+E Merger?	
H36442_1247	0.555	21.40	Sc:p	
H36439_1250	0.557	20.84	Pec/Merger?	
H36517_1353	0.557	21.08	Sp	
H36452_1142	0.558	24.00	“Tadpole”	
H36555_1359	0.559	23.74	Sbc(p?)	Edge-on, Asymmetric?
H36519_1400	0.559	23.03	Sbcp	Edge-on, Asymmetric

Table 1—Continued

ID ^a	Redshift ^b	R^c	Classification	Comments
		(Mag)		
H36534_1234	0.560	22.78	Sb/Ir	Multiple nuclei
H36571_1225	0.561	22.36	Scp	One-armed spiral
H37005_1234	0.563	21.43	E0	
H36554_1402	0.564	23.08	Sc/Ir	Edge-on
H36413_1141	0.585	21.91	Sa	
H36389_1219	0.609	22.14	Pec	
H36471_1414	0.609	23.92	E5 + E1	Spectrum probably refers to combined light
F36244_1454	0.628	20.34	E2	
F36249_1252	0.631	22.76	Sab/S0	
F36384_1312	0.635	22.27	Sabp	Asymmetric
F37163_1432	0.635	22.50	Sbp	Asymmetric
F36287_1357	0.639	23.05	Sa:	
F36247_1510	0.641	20.41	Sab	Rudimentary spiral structure
H36538_1254	0.642	20.95	(proto?)Sc	
F36248_1438	0.642	21.59	E1	
F36254_1519	0.642	21.82	Sbp	Asymmetric
F36481_1102	0.650	22.58	Sb	
F37080_1246	0.654	21.80	Sap	Asymmetric

Table 1—Continued

ID ^a	Redshift ^b	R^c	Classification	Comments
		(Mag)		
F36250_1341	0.654	24.32	E0/Star	
F37072_1214	0.655	22.19	Sab	
F37213_1120	0.656	22.22	S(B?) _c	
F37060_1340	0.672	23.25	S:	
F37171_1122	0.676	22.98	E1/Star	
H36471_1213	0.677	24.63	Sap + Sa/E3	Asymmetric envelope, spectrum probably refers to combined light
F36588_1434	0.678	20.85	Sb:	
H36459_1201	0.679	23.88	S:p	Edge-on
H36502_1245	0.680	21.74	E3/S0	
F36362_1319	0.680	22.20	Sb:p	
F36580_1137	0.681	23.00	E1	
H36475_1252	0.681	24.26	Sbp	Asymmetric
F36481_1002	0.682	21.92	Sbp	
H36586_1221	0.682	23.40	E3p	Non-elliptical isophotes
F36278_1449	0.680	21.64	Sa	
F36243_1525	0.682	22.78	E2/Sa	
F36454_1523	0.683	22.06	E4	

Table 1—Continued

ID ^a	Redshift ^b	R^c	Classification	Comments
		(Mag)		
F36499_1058	0.684	22.63	Sp	Arms under-developed
F37113_1545	0.692	22.43	Ir	
F37069_1208	0.693	24.13	E0/Sa	
F36290_1346	0.693	23.02	E2	
F36427_1503	0.698	23.17	Ir/Pec	Edge-on
F36415_0902	0.713	22.31	Sc:	
F37017_1143	0.744	22.10	Sa	
F37020_1517	0.744	23.56	Sb:	
F37036_1353	0.745	21.63	Sb:	
F37108_1059	0.747	24.25	? + ?	Combined spectrum of two LSB objects
F36297_1329	0.748	23.03	S:p	Edge-on
F36522_0957	0.750	23.07	Sabp	Asymmetric
H36498_1242	0.751	24.38	Ir	Edge-on
F36275_1418	0.751	22.37	Sb	Edge-on, Spectrum might refer to Ir? companion
H36436_1218	0.752	22.56	Sa	
F37074_1356	0.752	23.65	E2/Sa	
H36494_1406	0.752	21.95	Sa	
F37058_1317	0.753	21.95	Sc:p	No spiral arms
H36487_1318	0.753	22.87	proto-Sc	

Table 1—Continued

ID ^a	Redshift ^b	R^c	Classification	Comments
		(Mag)		
F37061_1332	0.753	21.85	Sbp	No spiral arms
F36297_1324	0.758	23.25	Sap	Binary nucleus ?
F36299_1440	0.762	22.81	Sa:p	
F36598_1449	0.762	21.62	Merger	
H36438_1142	0.765	21.26	E/Sa	Asymmetric envelope
F36379_0922	0.767	21.43	S(B?)b(p?)	Earliest phase of bar formation?
F37115_1042	0.778	21.97	Sbcp	
F37015_1129	0.779	21.45	Pec/Merger	Binary nucleus ?
F37192_1143	0.784	22.81	Sbc	
F37083_1320	0.785	22.86	“Tadpole”	
F37222_1124	0.786	22.33	Sa	
F37088_1214	0.788	23.90	E0/Star	
F37105_1141	0.789	21.20	Sbcp	No spiral arms
H36555_1245	0.790	23.08	Sbcp	Rudimentary spiral structure
F36299_1403	0.793	21.97	Merger	Merger of E0t + ?
F36270_1509	0.794	21.60	E2	
F36194_1428	0.798	22.60	Pec	
F37007_1107	0.801	22.94	Sab:	

Table 1—Continued

ID ^a	Redshift ^b	R^c	Classification	Comments
		(Mag)		
F36175_1402	0.818	21.73	Pec	
H36503_1418	0.819	23.41	Sbp	
F37167_1042	0.821	21.59	Ir/Merger	
F37141_1044	0.821	22.32	E2	
F37083_1252	0.838	22.20	Sbp	No spiral arms, spectrum may include Sb: companion
F37083_1514	0.839	21.62	Sp	
F37065_1512	0.840	22.94	E0/Star	
F37064_1518	0.840	22.22	?	Asymmetric
F37105_1116	0.841	23.60	Sb(p?)	
F36447_1455	0.845	22.97	Pec	
F36417_0943	0.845	22.51	Sb	
F36425_1121	0.845	23.03	Sbp	
F36343_1312	0.845	23.15	Pec/Merger?	
F36336_1319	0.845	21.78	Sep	No spiral arms
F36420_1321	0.846	23.95	Sap	Asymmetric envelope
F36341_1305	0.847	24.24	Sb:	
F36398_1249	0.848	21.53	Sa:	Nucleus too small for class

Table 1—Continued

ID ^a	Redshift ^b	R^c	Classification	Comments
		(Mag)		
F36176_1408	0.848	22.55	Sp	
H36431_1242	0.849	22.34	E2	
F36570_1511	0.849	23.50	E1:	
F36541_1514	0.849	22.84	Pec	
H36504_1315	0.851	23.41	Sbp	
H36540_1354	0.851	22.72	Sc?	
F36462_1527	0.851	22.11	Ir	
F36539_1606	0.851	22.84	Pec	Non-elliptical isophotes
F36589_1208	0.853	22.32	Sbp	Off-center nucleus
F37114_1054	0.855	22.44	Sb	
F37089_1202	0.855	22.90	Scp	Knots but no arms
F37129_1028	0.858	22.62	Pec:	Edge-on
F37096_1055	0.858	23.16	Pec	
F37041_1239	0.861	23.16	Pec	
F36472_1628	0.873	21.69	Sa	
F36408_1054	0.875	22.61	Merger?	
H36441_1240	0.875	23.39	Pec	
F36287_1239	0.880	22.11	Sa:	

Table 1—Continued

ID ^a	Redshift ^b	R^c	Classification	Comments
		(Mag)		
H36408_1205	0.882	22.94	E1p	Asymmetric envelope
F36482_1507	0.890	22.38	Sa	
F37029_1427	0.898	23.67	E:1	
H36461_1246	0.900	22.86	E1	
F37058_1153	0.904	21.22	Scp	
H36386_1233	0.904	24.04	Sab	Edge-on
F36469_0906	0.905	23.84	Sbp	Asymmetric, image too small to classify with confidence
H36501_1216	0.905	23.06	proto-Sbc?	Edge-on
F37176_1113	0.906	22.01	E3/Sa	
F37086_1128	0.907	22.23	Merger	
F37196_1256	0.909	23.31	Sab	Asymmetric
F37180_1248	0.912	22.89	Sbc	
F36468_1540	0.912	22.23	Sc(p?)	
F37003_1616	0.913	22.33	Merger?	
F37001_1615	0.914	22.83	Sab	
F36518_1125	0.919	21.62	Ir/Merger?	
H36566_1220	0.930	23.15	E2p	

Table 1—Continued

ID ^a	Redshift ^b	R^c	Classification	Comments
		(Mag)		
F37133_1054	0.936	21.87	E2p	Asymmetric
F36522_1537	0.936	22.74	E0/Star	
F36459_1101	0.936	22.77	E0	
F37078_1605	0.936	21.88	proto-Sc	
F36444_1052	0.937	23.50	“Tadpole?”	Might also be an asymmetric Sab
F37018_1509	0.938	22.20	Sbp	
F36532_1116	0.942	22.08	Proto-Sc?	
F36529_1508	0.942	22.84	E0/Star	
H36396_1230	0.943	24.40	E/Sa(p?)	
H36384_1231	0.944	22.87	Amorphous	Edge-on, off center nucleus ?
F36465_1049	0.945	23.70	Sa?	
H36555_1249	0.950	23.53	proto-Sc	
H36551_1303	0.952	24.29	E3	
H36576_1315	0.952	22.94	Pec/Merger	
H36490_1221	0.953	22.59	Pec	Nucleus + 4 bright knots
F36524_0919	0.954	22.81	E3	
F36502_1127	0.954	22.88	Sbcp	
F36520_1059	0.955	23.67	S	

Table 1—Continued

ID ^a	Redshift ^b	R^c	Classification	Comments
		(Mag)		
H36486_1328	0.958	23.14	Pec/Merger	
H36477_1232	0.960	23.80	Sa	
F36366_1346	0.960	20.32	E0	
H36492_1148	0.961	23.26	Sa:p	Asymmetric
H36493_1155	0.961	23.36	E2	
F36364_1237	0.961	22.94	Sbp	
F36486_1141	0.962	22.21	Sbt	
H36483_1214	0.962	23.87	S(B)bct	
H36463_1404	0.962	21.69	E0	Embedded in large shell
F37224_1216	0.963	22.23	Sb(t?)	Part of multiple interacting system
H36554_1310	0.968	22.86	E1	
F37058_1423	0.970	22.48	Sb:	
F37055_1129	1.001	22.37	Sap	
H36432_1148	1.010	23.10	Sbp	Smooth disk with little star formation ?
H36408_1203	1.010	23.49	Ir	Edge-on
H36461_1142	1.013	21.52	proto-Sc	
F37000_1605	1.013	22.46	Sc:	On edge of image
F37154_1212	1.014	23.25	Ep	

Table 1—Continued

ID ^a	Redshift ^b	R^c (Mag)	Classification	Comments
H36400_1207	1.015	22.75	E0	
F36411_1314	1.017	23.08	Sap	Asymmetric
F36497_1106	1.018	23.37	Pec	
H36444_1142	1.020	24.30	Pec/Merger	
F37159_1213	1.020	23.27	Sbcp	
F36583_1214	1.020	23.79	E2	
F36595_1153	1.021	22.54	Sap(t?)	Asymmetric
H36443_1133	1.050	21.96	E1	
F37046_1415	1.050	23.97	Sab:	
F36296_1420	1.055	24.00	E0/Star	
H36467_1144	1.060	24.23	proto-Sc	
F37026_1216	1.073	24.04	Sabp	Asymmetric
F37143_1221	1.084	24.12	E:2	Image too small to classify with confidence
H36519_1332	1.087	23.59	Sap	

^aNames are Habcde_fghi for objects in the HDF, where the object’s J2000 coordinates are 12 ab cd.e +62 fg hi. The initial letter is “F” for objects in the flanking fields.

^bRedshifts are from Cohen *et al.* (2000) or Cohen (2001).

^c R magnitudes are from Hogg *et al.* (2000).

Table 2. FREQUENCY DISTRIBUTION OF GALAXY TYPES

z	$n(z)$	E ^a	Sa + Sab	Sb + Sbc ^b	Sc + Sc/Ir ^b	Ir	Pec	P/Mer	Mer	?
0.20 – 0.29	4	0	1	1	0	2	0	0	0	0
0.30 – 0.39	7	0	1	2.5	1	0.5	1	0	1	0
0.40 – 0.49	25	4	4	5	4 + (1)	0	2	1	0	0
0.50 – 0.59	24	5	2	5	3	2.5	0	1	1	1
0.60 – 0.69	37	14	7	7	1 + (1)	1.5	1	0	0	0
0.70 – 0.79	32	4	7	8	2 + (1)	1	1	1	2.5	2
0.80 – 0.89	41	7	7	9 + (1)	3	1.5	9	1	2	1
0.90 – 0.99	43	14	5	11	2 + (2)	0.5	1	2	2.5	0
1.00 – 1.09	20	6	6	0	1 + (1)	1	1	1	0	0
Total	233	55	40	48.5 + (1)	17 + (6)	10.5	16	7	9	4

^aIncludes E, E0/Star, E/Sa, S0 and S0/Sa

^bNumbers in parentheses refer to objects that were classified as proto-Sb or proto-Sc

REFERENCES

- Abraham, R. G., 1999, *Ap&SS*, 269–70, 323
- Abraham, R. G., Merrifield, M. R., Ellis, R. S., Tanvir, N. R., & Brinchmann, J., 1999, *MNRAS*, 308, 569
- Abraham, R. G. & van den Bergh, S., 2001, in preparation
- Binchmann, J. *et al.* 1998, *ApJ*, 499, 112
- Bothun, G. D., 2000, *S&T*, May, 37
- Carollo, C. M. & Lilly, S. J., 2001, *ApJ*, 548, L153
- Cohen, J. G., 2001, *AJ*, in press (see Astro-ph/0101251)
- Cohen, J. G., 2000, to appear in *Deep Fields*, ed. S.Cristiani, A.Renzini & R.E.Williams, ESO Astrophysics Symposia, Springer-Verlag, Heidelberg (see Astro-ph/0012004)
- Cohen, J. G., Hogg, D. W., Blandford, R. D., Cowie, L. L., Hu, E., Songaila, A., Shopbell, P. & Richberg, K., 2000, *ApJ*, 538, 29
- Drozdosky, I. O., Schulte-Ladbeck, R. E., Hopp, U., Crone, M. M. & Greggio, L., 2001, *ApJ*, in press (see Astro-ph/0102452)
- Eskridge, P. B. *et al.* 2000, *AJ*, 119, 536
- Guzmán, R., Gallego, J., Koo, D. C., Phillips, A. C., Lowenthal, J. D., Faber, S. M., Illingworth, G. D., & Vogt, N. P., 1997, *ApJ*, 489, 559
- Hubble, E., 1936, *The Realm of the Nebulae*, (New Haven: Yale University Press), p.45
- Lilly, S. J., Tresse, L., Hammer, F., Crampton, D., & Le Fèvre, O., 1995, *ApJ*, 455, 108

Noguchi, M., 1998, *Nature*, 392, 253

Phillips, A. C., Guzmán, R., Gallego, J., Doo, D. C., Lowenthal, J. D., Vogt, N. P., Faber, S. M., & Illingworth, S.D., 1997, *ApJ*, 489, 543

Sandage, A. & Tammann, G. A., 1981, *A Revised Shapley-Ames Catalog of Bright Galaxies*, (Washington: Carnegie Institution)

van den Bergh, S., 1960a, *ApJ*, 131, 215

van den Bergh, S., 1960b, *ApJ*, 131, 558

van den Bergh, S., 1960c, *Pub. David Dunlap Obs.*, 2, 159

van den Bergh, S., 1989, *AJ*, 97, 1556

van den Bergh, S., 1998, *Galaxy Morphology and Classification*, (Cambridge: Cambridge Univ. Press)

van den Bergh, S., Abraham, R. G., Ellis, R. S., Tanvir, N. R., Santiago, B. X. & Glazebrook, K. G., 1996, *AJ*, 112, 359

van den Bergh, S., Cohen, J. G., Hogg, D. W., & Blandford, R., 2000, *AJ*, 120, 2190

Williams, R. E. *et al.* 1996, *AJ*, 112, 1335

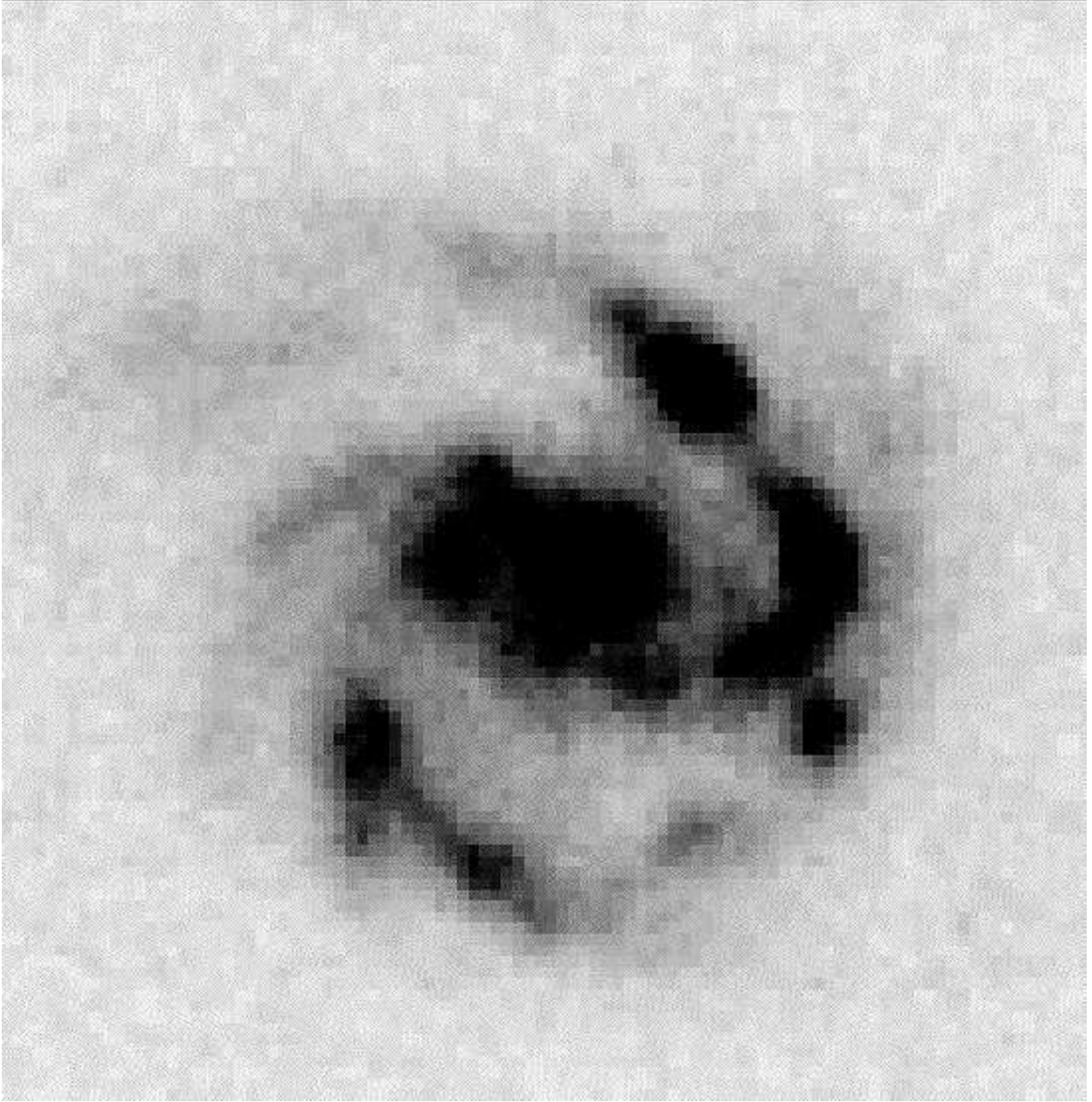


Fig. 1.— Example of what is interpreted as a proto-Sc galaxy. Note the rather chaotic spiral structure and very patchy arm morphology of H36461_1142 at $z = 1.01$. (Original figures have slightly more contrast.)

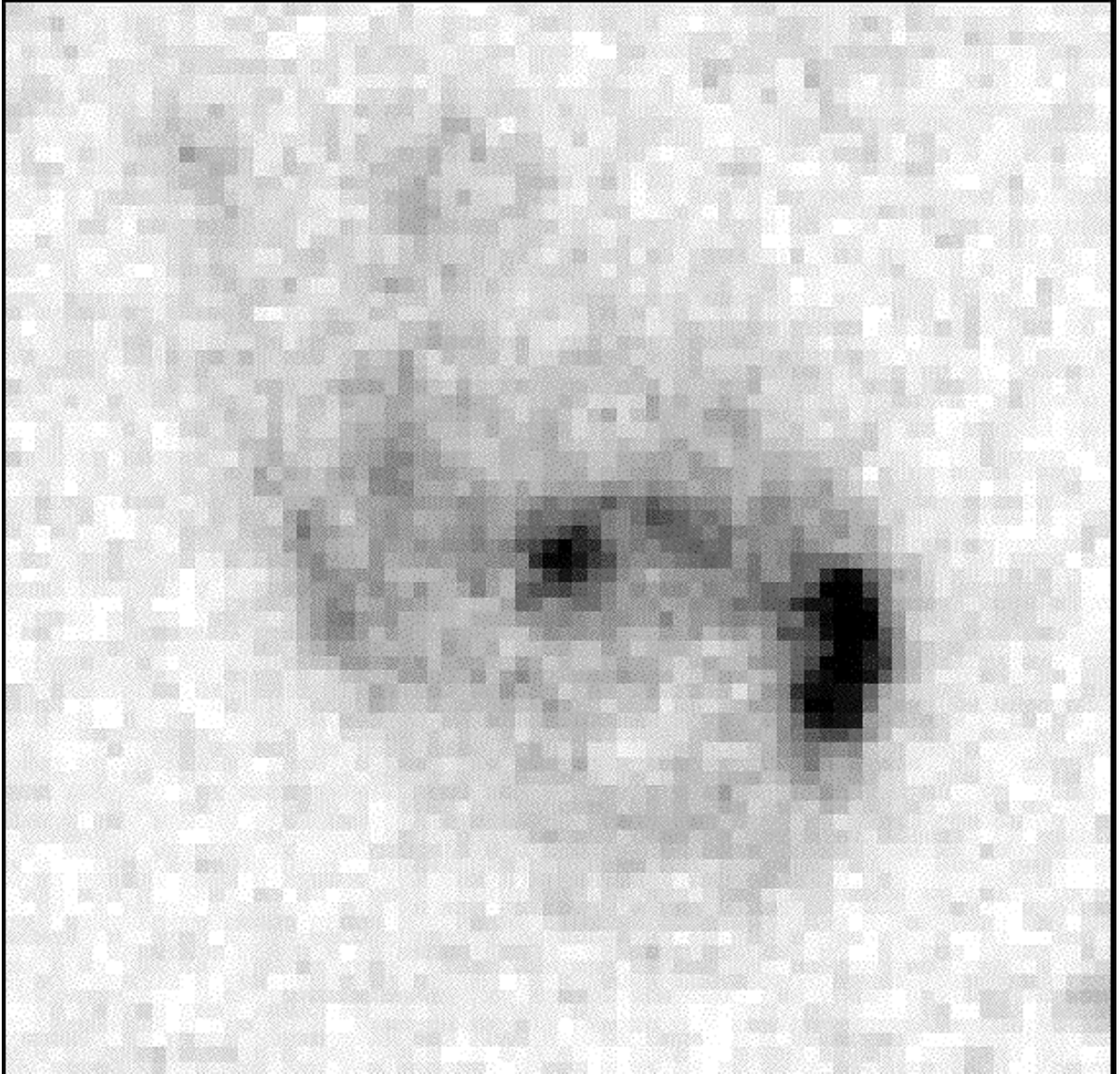


Fig. 2.— This spiral(?) (H36467_1144) might be interpreted as either a proto-Sc with a very patchy arm structure, or as the product of a recent merger. Kinematical studies of this object at $z = 1.06$ will be required to distinguish between these two alternatives. (Original figures have slightly more contrast.)

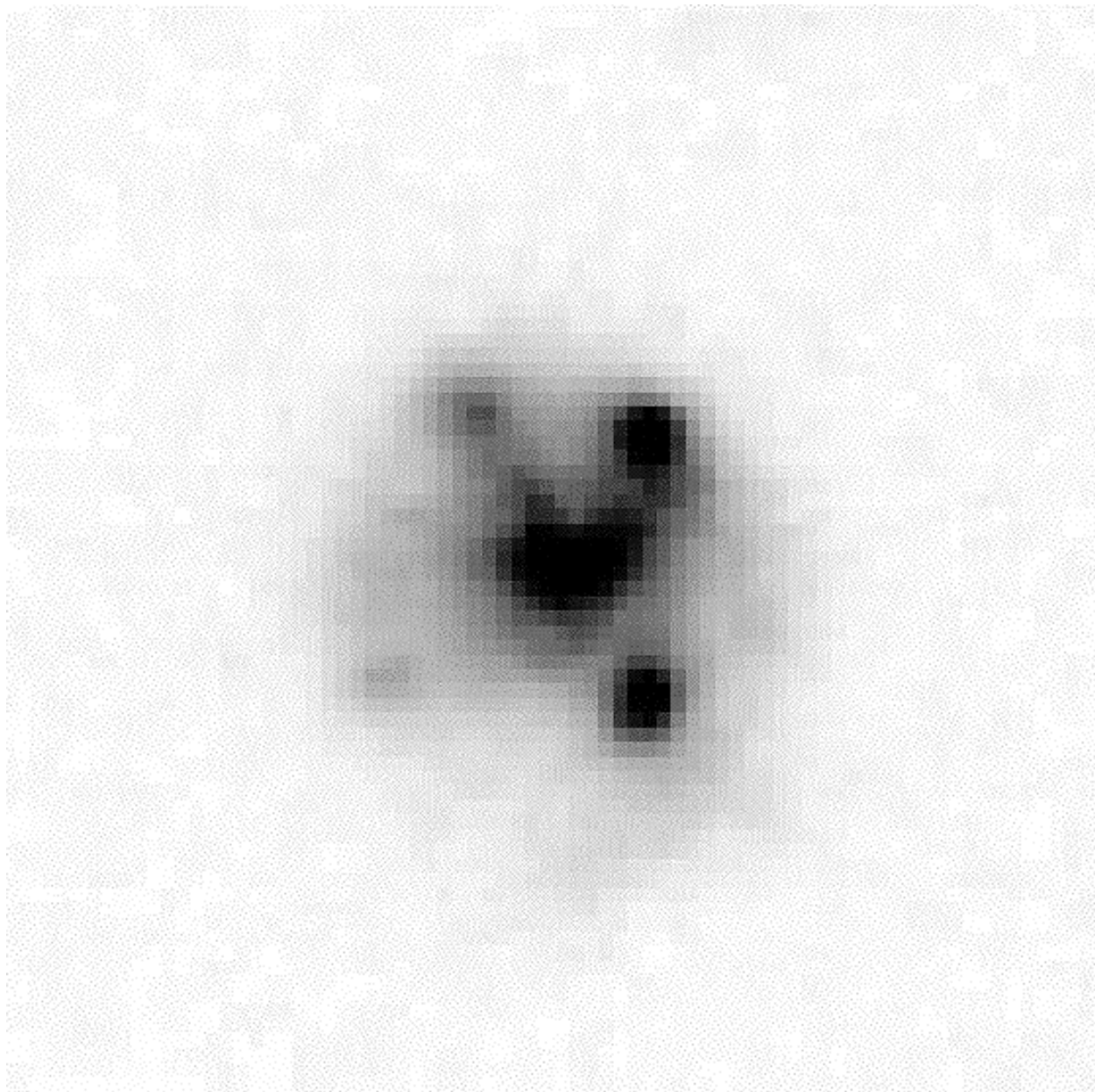


Fig. 3.— This peculiar disk galaxy (H36490_1221) at $z = 0.953$ consists of a disk in which five bright knots, one of which might be the nucleus, are embedded. No spiral structure appears to have developed yet in this object. (Original figures have slightly more contrast.)